

# AF6 preserves the continuity of epithelial cell sheets during wound closure by stabilizing cell adhesion through its interaction with actin cytoskeleton

Lorger, Mihaela and K. Moelling

Institute of Medical Virology, University of Zurich

## Abstract

AF6 (AF6 isoform 1; AF6i1) is a multidomain protein localized at the cell-cell contacts and involved in the regulation of signaling cascades via the small GTPases Ras and Rap1. We cloned a new isoform of human AF6 protein, AF6 isoform 3 (AF6i3), which contains an additional F-actin binding site at its C-terminus (Fig. 1). The AF6i3 analogue in *Drosophila* (canoe) is essential for the dorsal closure in embryo and its rat analogue I-afadin for the adherens junctions assembly during embryogenesis. The non-transformed human epithelial breast cell line MCF10A expresses only the longer AF6 isoform. Stable expression of shRNA against AF6 (AF6 shRNA) resulted in approximately 90 percent reduction of the endogenous AF6 protein level in this cell line (Fig. 2A). Cells with reduced AF6 expression displayed an increased velocity of wound closure during the wound healing assay (Fig. 2B,C), which was due to the higher directionality of the cell movement into the wound and disability to retain the continuity of the epithelial cell sheet during migration (Fig. 3). Furthermore, the knock-down of AF6 resulted in a significantly reduced velocity of cell-cell contact formation during the calcium switch assay (Fig. 4). Two hours after the cell contact reformation was initiated by switch to a higher (2mM) calcium concentration, the AF6 knock-down cells displayed a significantly lower percentage of  $\beta$ -catenin, nectin-1 and E-cadherin positive cell-cell contacts (Fig. 4A,B,D,E). At the same time, length of the existing cell contacts was significantly shorter for the AF6 shRNA expressing cells (Fig. 4C).

In order to prove the AF6-dependence of the described phenotype and to screen for the involved AF6 domains, we generated AF6 mutant constructs (AF6i3, AF6i1, AF6 $\Delta$ RBD2 and AF6 $\Delta$ PDZ) resistant to degradation by AF6 shRNA, which enables their expression in AF6 knock-down cells (Fig. 5A). The expression of the mutant AF6i3 construct in AF6 shRNA expressing cells indeed resulted in decreased wound closure (Fig. 5B) and increased velocity of cell contact formation (Fig. 6), reflecting the wild type phenotype and thus confirming the AF6-dependence of both processes. The AF6 $\Delta$ RBD2 and AF6 $\Delta$ PDZ constructs expressed in AF6 knock-down cells also resulted in wound closure reminiscent of the wild type (Fig. 5B). Thus, these two domains do not seem to be involved in this process. By contrast, the AF6i1 expressing AF6 knock-down cells still displayed an increased velocity of wound closure, similar to the AF6 knock-down cells (Fig. 5B). Furthermore, during the calcium switch assay only the AF6i3 was able to increase the velocity of cell-cell contact formation to the level observed for the control. At the same time the length distribution of cell contacts was similar to the control (Fig. 6C). By contrast, the expression of AF6i1 only partially reconstituted the wild type velocity of cell contact formation with  $\beta$ -catenin positive cell-cell contacts being significantly shorter (Fig. 6A-C).

In confluent monolayer of MCF10A cells the AF6i1 showed similar localization at the cell-cell contacts as the AF6i3 (Fig. 5C). Thus, although the F-actin binding site is not necessary for the AF6 localization at cellular junctions, the interaction of AF6 protein with F-actin seems to be essential for the establishment and maintenance of cell-cell contacts, thereby contributing to the epithelial sheet integrity during wound closure. Therefore, from the two isoforms, apparently only the isoform 3 fulfills the biological function in cell-cell adhesion.

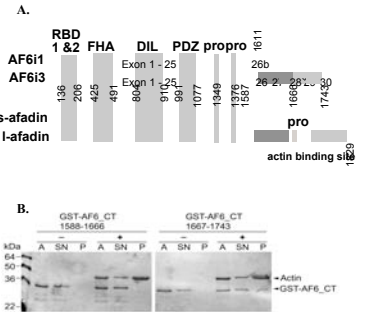


**Fig. 1. (A)** Domain structure of the AF6 and afadin isoforms. The amino acid positions of individual domains are annotated. The exon numbers are shown for the AF6 isoform 3 in comparison to the isoform 1. R1A12: Ras associating domain; FHA: forkhead associated domain; DIL: dilute domain; PDZ: PSD-95/Dlg-1/ZO-1 domain; pro: proline rich domain. **(B)** In vitro F-actin cosedimentation assay: GST fusion protein of C-terminal AF-6 isoform 3 fragments (amino acids 1588-1666 and 1667-1743) were incubated with F-actin (+) or (-) for 1 hour at 4°C. The F-actin and associated proteins were pelleted via centrifugation at 100,000 g for 1 hour. The reaction mixture before centrifugation (A), the supernatant (SN) and the pellet (P) were analysed on coomassie blue stained SDS polyacrylamide gel. Only the GST fusion protein of the C-terminal AF-6 isoform 3 fragment harboring the amino acids 1667-1743 cosedimented with F-actin (lane P+), thus indicating the presence of F-actin binding site at the very C-terminus of the longer AF-6 isoform.

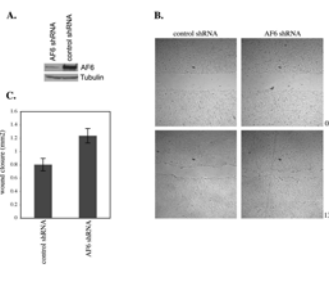


**Fig. 2. Knock-down of AF6 in MCF10A cells and wound healing assay. (A)** Western blot analysis of the MCF10A whole cell lysates expressing the AF6 shRNA (left panel) or control shRNA against GFP protein (right panel). Anti-AF6 antibody was used for detection. **(B)** Light microscopy pictures of the MCF10A cells during the wound healing assay. The assay was performed with cells expressing the AF6 shRNA (right panel) or the control shRNA (left panel). Cell migration was initiated by wounding the cell monolayer in medium containing 10 ng/mL EGF. Pictures were taken immediately after the wound was introduced (0h; upper panels) and 13 hours after the initiation of migration (13h; lower panels). **(C)** Graphic representation of the wound closure during the wound healing assay shown in B. Wound closure 13 hours after the wound introduction is depicted. Standard deviations are derived from three independent experiments.

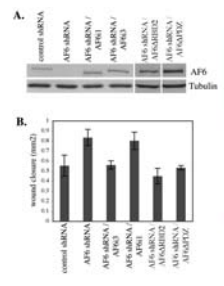


**Fig. 5. AF6 deletion mutants in wound healing assay. (A)** Western blot analysis showing the expression of shRNA resistant AF6 constructs (AF6i1, AF6i3, AF6 $\Delta$ RBD2 and AF6 $\Delta$ PDZ) in MCF10A cells stably expressing AF6 shRNA. The detection was performed with anti-AF6 (upper panel) or anti-tubulin antibody (lower panel). **(B)** Graphic representation of wound closure during the wound healing assay for MCF10A cells expressing the control shRNA, the AF6 shRNA or coexpressing the AF6 shRNA and one of the shRNA resistant AF6 constructs (AF6i1, AF6i3, AF6 $\Delta$ RBD2 and AF6 $\Delta$ PDZ) 13 hours after wound introduction. **(C)** Immunofluorescence pictures of confluent MCF10A cell monolayers expressing the control shRNA, the AF6 shRNA, the AF6 shRNA and AF6i1 or AF6i3 construct, as well as AF6 shRNA and the AF6i3 construct. The detection was performed with anti-AF6 antibody.

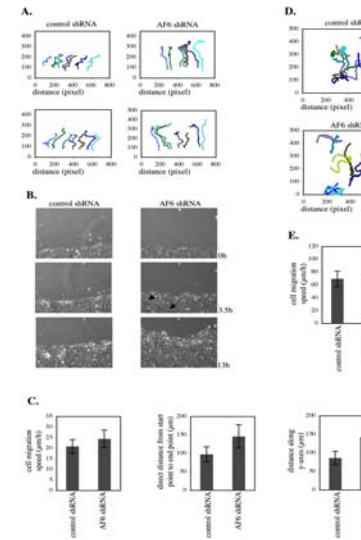


**Fig. 3. Time lapse analysis of the epithelial sheet movement during wound healing assay (A-C) and of single cells (D,E).** **(A)** Representative trajectories of individual cells within the MCF10A cell monolayer during wound healing assay, followed for 13 hours. Two independent experiments (upper and lower panels) each showing trajectories for 7 cells per sample are depicted. **(Left panel)** MCF10A cells expressing the control shRNA. **(Right panel)** MCF10A cells expressing the AF6 shRNA. Three different time points during the wound closure (0h, 3.5h and 13h). **(Left panel)** MCF10A cells expressing the control shRNA. **(Right panel)** MCF10A cells expressing the AF6 shRNA. Disturbances of the cell-cell contacts within the monolayer of migrating MCF10A cells expressing the AF6 shRNA are marked by arrows. **(C)** Graphic representation of the cell migration speed (left panel), direct distance from the cell track start point to the cell track end point (middle panel) and the distance from the track start point to the track end point along the migration axes (right panel). Data are derived from two independent experiments shown in A. Bulges represent the mean values of the 14 trajectories. Standard deviations are represented by bars. **(D)** Time lapse analysis of the single cell movement. Representative trajectories of the MCF10A cells expressing the control shRNA (upper panel) or the AF6 shRNA (lower panel), followed for 4.5 hours, showing 10 cells per sample. **(E)** Graphic representation of the single cell migration speed derived from the data shown in D. Bulges represent the mean value for 10 cells. Standard deviations are represented by bars.

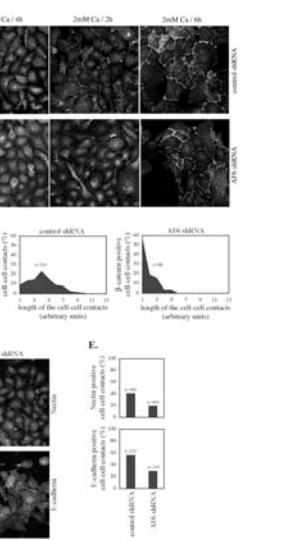


**Fig. 4. Calcium switch assay. (A)** Anti- $\beta$ -catenin staining of MCF10A cells. The nearly confluent MCF10A cells (left panel) expressing the control- (upper panel) or the AF6 shRNA (lower panel) were incubated in the presence of 5 mM EGTA for 4 hours in order to disturb cell junctions (2 $\mu$ M Ca / 4h). The reformation of cell-cell contacts 2 and 6 hours after switch to the higher calcium concentration (2mM Ca) is depicted. **(B)** Graphic representation of the percentage of  $\beta$ -catenin positive cell-cell contacts 2 hours after the switch to the higher calcium concentration (see A, 2mM Ca / 2h). Standard deviations are derived from two independent experiments. Numbers of counted cell-cell contacts are indicated (n). **(C)** Length distribution of  $\beta$ -catenin positive cell-cell contacts 2 hours after the switch to the higher calcium concentration. Lengths of all  $\beta$ -catenin positive cell-cell contacts from two independent experiments were measured (n indicates the exact numbers). The resulting values were grouped into 13 categories. Graphs represent the percentage of cell contacts within each length category for the control (left panel) and the AF6 shRNA expressing cells (right panel). **(D)** Anti-Nectin-1 (upper panel) and anti-E-cadherin staining (lower panel) of MCF10A cells during calcium switch assay, 2 hours after the switch to the higher (2mM) calcium concentration. **(Left panel)** control shRNA. **(Right panel)** AF6 shRNA. **(E)** Graphic representation of the percentage of Nectin-1 positive- (upper panel) and E-cadherin positive cell-cell contacts (lower panel). Data are derived from one experiment. The numbers of counted cell-cell contacts are indicated (n).

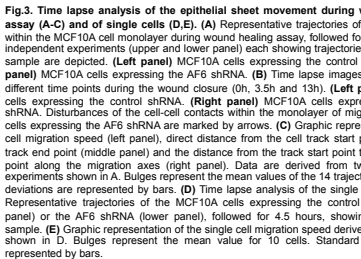


**Fig. 6. Calcium switch assay with MCF10A AF6 knock-down cells expressing the shRNA-resistant AF6i1 and AF6i3 constructs. (A)** Anti- $\beta$ -catenin staining of MCF10A cells. The nearly confluent MCF10A cells (left panel) expressing the control shRNA (upper panel), the AF6 shRNA (second panel), the AF6 shRNA and the AF6i1 (third panel) as well as AF6 shRNA and AF6i3 (lower panel) were incubated in the presence of 5 mM EGTA for 4 hours (2 $\mu$ M Ca / 4h) in order to disturb cell junctions. The reformation of cell-cell contacts 2 and 6 hours after switch to the higher calcium concentration (2mM Ca) is depicted. **(B)** Graphic representation of the percentage of  $\beta$ -catenin positive cell-cell contacts 2 hours after the switch to the higher calcium concentration (see A, 2mM Ca / 2h). Data are derived from one experiment. The numbers of counted cell-cell contacts are indicated (n). **(C)** Length distribution of  $\beta$ -catenin positive cell-cell contacts 2 hours after the switch to the higher calcium concentration. Lengths of all  $\beta$ -catenin positive cell-cell contacts were measured (n indicates the exact numbers). The resulting values were grouped into 13 categories. Graphs represent the percentage of cell contacts within individual length categories for the control, the AF6 shRNA expressing cells, as well as the cells coexpressing the AF6 shRNA and the AF6i3, or AF6 shRNA and AF6i1.

**Fig. 6. Calcium switch assay with MCF10A AF6 knock-down cells expressing the shRNA-resistant AF6i1 and AF6i3 constructs. (A)** Anti- $\beta$ -catenin staining of MCF10A cells. The nearly confluent MCF10A cells (left panel) expressing the control shRNA (upper panel), the AF6 shRNA (second panel), the AF6 shRNA and the AF6i1 (third panel) as well as AF6 shRNA and AF6i3 (lower panel) were incubated in the presence of 5 mM EGTA for 4 hours (2 $\mu$ M Ca / 4h) in order to disturb cell junctions. The reformation of cell-cell contacts 2 and 6 hours after switch to the higher calcium concentration (2mM Ca) is depicted. **(B)** Graphic representation of the percentage of  $\beta$ -catenin positive cell-cell contacts 2 hours after the switch to the higher calcium concentration (see A, 2mM Ca / 2h). Data are derived from one experiment. The numbers of counted cell-cell contacts are indicated (n). **(C)** Length distribution of  $\beta$ -catenin positive cell-cell contacts 2 hours after the switch to the higher calcium concentration. Lengths of all  $\beta$ -catenin positive cell-cell contacts were measured (n indicates the exact numbers). The resulting values were grouped into 13 categories. Graphs represent the percentage of cell contacts within individual length categories for the control, the AF6 shRNA expressing cells, as well as the cells coexpressing the AF6 shRNA and the AF6i3, or AF6 shRNA and AF6i1.